Journal of Advanced Chemical Engineering
ISSN: 2090-4568

Namdeo et al., J Adv Chem Eng 2018, 8:2
DOI: 10.4172/2090-4568.1000189

Research Article Open Access

Preparation and Application of Magnetic Materials for the Removal of As (III) from Aqueous Solutions

Mini Namdeo* **and Ankita Mathur**

Centre of Excellence- Nanotechnology, Indian Institute of Technology Roorkee, Uttarakhand, India

***Corresponding author:** Mini Namdeo, Centre of Excellence-Nanotechnology, Indian Institute of Technology, Roorkee, Uttarakhand, India, Tel: +917060214491; Email: mini.namdeo@gmail.com

Received date: October 5, 2018; **Accepted date:** October 17, 2018; **Published date:** October 24, 2018

Abstract

Higher environmental standards have made for the removal of arsenic from water, an important problem for environmental engineering. Iron oxide is a particularly interesting sorbent to consider for this application. Its magnetic properties allow relatively routine dispersal and recovery of the adsorbent into and from groundwater or industrial processing facilities; in addition, iron oxide has strong and specific interactions with both As (III) and As(V). Finally, this material can be produced with nanoscale dimensions, which enhance both its capacity and removal. The present study focuses on iron-oxide based complexes that were found to adsorb arsenic from water. Their composition, morphology, magnetic behaviour and potential were studied by Fourier Transform Infra-Red (FTIR) Spectroscopy, X-Ray Diffraction (XRD), Field Emission Scanning Electron Microscopy (FESEM), Transmission Electron Microscopy (TEM), Zeta potential and Vibrating Sampling Magnetometer (VSM). Arsenic concentrations were recorded by Inductively Coupled Plasma-Mass Spectrometry (ICP-MS). Finally, the particles were also investigated for their antimicrobial properties that can be used against gram positive and gram-negative bacteria. The study suggests that among various iron oxide sorbents magnetite chitosan beads provides a low cost, fast and effective method for removal of arsenic from potable water, and thus making it suitable for drinking purpose.

Keywords: Magnetite; Chitosan; Arsenic; Adsorption; Antibacterial activity

Introduction

The removal of toxic and polluting heavy metal ions from industrial effluents, water supplies and mine waters has received much attention in recent years. Arsenic (As)-contaminated drinking water is a major problem around the world. Countries such as Bangladesh, India, Vietnam, Mexico, Argentina, Chile, Hungary, Romania, and the United States face significant challenges in meeting the newly lowered standards for Arsenic in drinking water [1]. Several methods of As removal are already available including precipitation, adsorption, ion exchange, solvent extraction, nanofiltration, foam flotation, and biological sequestration [2]. Adsorption is a low cost, efficient and easy method to remove effluents from water [3]. It is simple, environmental- friendly, requires less skill and can treat water of high quality [4]. Various adsorbents have been used so far for removal of arsenic, including zirconium oxide [5], manganese oxide [6], titanium oxide [7], orange juice [8], human hairs [9] etc. Nanoscale nickel/nickel borides were also effective adsorbents for mitigating arsenic from drinking water [10]. Various low-cost adsorbents have been synthesized like bagasse fly ash (BFA), by-product of sugarcane industry; it can remove up to 95% arsenite and arsenate ions from water by column and batch modes [11]. Similarly, a biochar was prepared by pyrolysing hematite and pinewood biomass and was found effective in removing arsenic [12]. Many papers have been published demonstrating that bulk iron oxides have a high affinity for the adsorption of arsenite and arsenate [13,14]. As (III) can form inner sphere monodentate or bidentate-binuclear complexes with iron oxides. Extended X-ray absorption fine structure spectroscopy has provided direct evidence for inner sphere adsorption of arsenite and arsenate on iron oxides [15-17]. Chitosan as a natural polysaccharide derived from renewable sources is one of the most studied biopolymers with significant potential for different applications including medical, pharmaceutical and biotechnological applications because of its good biocompatibility, biodegradability and low toxicity [18]. The appropriate involving of magnetic material in chitosan-based materials would enlarge the areas of its possible application, e.g., for fast and easy separation of microorganisms, as magnetic drug-targeting carriers, contrast enhancement agents in magnetic resonance imaging, etc. That is why chitosan has recently attracted increasing interest as carrier in magneto-sensitive materials. (one pot mag bead) Usually the potable water is free from the pathogenic organisms, however, in the public potable water systems presence of viruses, bacteria, fungi, and parasites is possible. Therefore, using copper and chitosan may also help in fighting the pathogenic organisms in the potable water. [19,20].

In present work, we demonstrate a comparative study of various Iron oxide nanoparticles on the adsorption behavior of Arsenic metal ion. In addition, we evaluate and compare their antibacterial activities against gram positive and gram-negative bacteria.

Experimental Work

Materials

Chitosan (Molecular weight 200 kDa, DA-80) was purchased from Hi-media. Other reagents such as Arsenic, ferrous chloride, ferric chloride, potassium sodium tartrate, ferric oxide red (hematite), copper sulphate pentahydrate, sodium hydroxide pellets, iron powder and formaldehyde were also purchased from Hi-Media and Merck, are used as received. The double distilled water was used throughout the investigations.

Synthesis of magnetic materials

Magnetite nanoparticles: Magnetite nanoparticles (Fe_3O_4) were prepared by chemical co-precipitation of Fe^{2+} and Fe^{3+} ions in aqueous solution of sodium hydroxide, followed by treatment under hydrothermal conditions [21]. Iron (II) chloride and Iron (III) chloride were dissolved in 1:2 molar ratio in distilled water and chemically precipitated at 40C by adding 30% NaOH (w/v) dropwise with constant stirring, at a controlled pH (10-10.4). The suspension was heated at 90C for one hour under continuous stirring and separated by centrifuging several times in water and then in ethanol at 200 rpm. This purification step was used to remove impurities from Fe_3O_4 nanoparticles. The particles were finally dried in vacuum at 70C.

Magnetic chitosan beads: For preparation of chitosan beads with in situ prepared nanosized magnetite, further denoted as CS-Fe_3O_4 (in situ), solution containing 40 ml of 0.4% chitosan solution in 0.4 M HCl.

0.05 M $FeCl_2$ and 0.1 M $FeCl_3$ was prepared. The obtained homogeneous solution was filtered and dropped through capillary (diameter 0.5 mm) into ammonium hydroxide precipitation bath (2.9 M NH_3), containing 0.026 M Na_2SO_3. The prepared CS-Fe_3O_4 (in situ) beads were kept in the precipitation bath for 24 h and then were repeatedly washed with deionized water to neutral reaction of the aqueous phase.

Cu coating on nanoparticles: Copper coated nanoparticles were synthesised by electroless method [22], which involves following steps: -

Activation of the particles surface: Magnetic chitosan beads were washed with acetone, followed by absolute ethanol. Acetone and ethanol acts as degreasing agent and removes all the dust and other contaminants.

Preparation of copper bath for coating of Magnetic Chitosan beads: Copper bath was prepared by adding 1:4 ratio of copper sulphate pentahydrate ($CuSO_4.5H_2O$), potassium sodium tartrate in preheated water at 70°C. Sodium hydroxide (NaOH) is used to adjust pH up to 10.8. Further above solution is followed to vigorous stirring. Add formaldehyde solution in 1:10 ratio, soon afterwards activated particles of Magnetic chitosan beads were added into the copper bath. Filter the precipitate and dry it.

Characterization

The crystal structure of the samples was studied using Bruker AXS D8 Advance powder X-Ray Diffractometer using Cu Kα as target (λ=1.54 Å) in the range 10-90 at a scan speed of 0.1per minute. The morphology, particle size and elemental composition analysis was performed by using transmission electron microscopy (TEM), Tecnai G2 20, field emission scanning electron microscope (FE-SEM) (Carl Zeiss Ultra Plus) equipped with energy dispersive X-ray detector (EDX), operating at an accelerating voltage of 15-20 kV. The chemical bonds were studied using Thermo Nicolet Fourier Transform Infrared (FTIR) spectrometer in the range 4000-400cm^{-1} using KBr pellets. The magnetic properties of the samples were studied by vibrating sample magnetometer (VSM) (model number 155, Princeton Applied research). On the other hand, stability of particles was evaluated by finding out their potential at neutral pH using Malvern Zeta Sizer. For antibacterial activity tests, 20 ml nutrient agar was poured in well-rinsed, autoclaved petri plates and allowed to solidify. 100 µl of fresh bacterial culture of both the strains was homogeneously spread on the solidified agar plates and 5 mg of iron oxide nanocomposites spread on plates. The plates were incubated at 37°C for 24 h. The zone size was determined by measuring the radius of the zone of inhibition by scale and divider.

As (III) uptake studies

Forty milliliters of As (III) solution of desired concentration was placed in different 125 ml Erlenmeyer flask containing 0.01 g of various iron oxide sorbents and was agitated in thermostatic water bath at 50 rpm for 3 h. At the end of experiment the sorbent was separated by filtration and supernatant was analyzed by ICP-MS (Perkin Elmer SCIEX ELAN DRC-e).

Result and Discussions

FTIR analysis

In Figure 1, (a-c) the bands at 3437 cm^{-1}, 1636 cm^{-1}, 1127 cm^{-1} and 617 cm^{-1} were involved in bonding. Band at 617 cm^{-1} represents the Fe-O-Fe vibrations. It is characteristic band of Fe_3O_4. Bands at 3437 cm^{-1} and 1636 cm^{-1} represent stretching and bending mode of O-H due to adsorption of water in sample [23]. In Figure 1, (c) band at 2360 cm^{-1} represents acylamino bonds in chitosan.

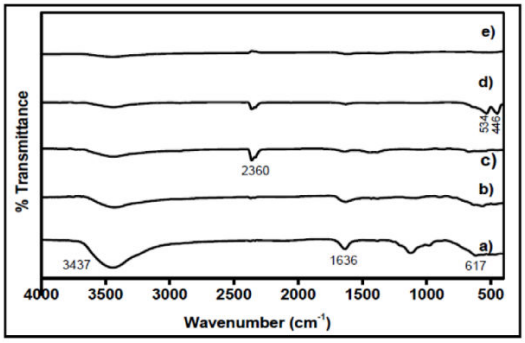

Figure 1: Showing FTIR Images of different Iron oxide composites: a) Fe_3O_4, b) Fe_3O_4-Cu, c) Fe_3O_4- Chitosan, d) Fe_2O_3- Cu, e) Fe-Cu.

Figure 1, (d) shows FTIR Image of Fe_2O_3 coated with copper, with bands at 3431, 2360, 1627, 534 and 446 cm^{-1}. Bands at 534 and 446 cm^{-1} correspond to Fe-O-Fe vibrations and were characteristic peak of Fe_2O_3. The rest bands are involved in bonding with copper.

Similarly, in Figure 1, (e) bands observed at 3430, 1630, 1380, 1109 cm^{-1} are involved in bonding with copper, and 747 and 517 cm^{-1} were characteristic peaks of Fe vibrations.

XRD analysis

Figure 2 projects the XRD images of all the samples. Figure 2, (a) shows the XRD pattern of Fe_2O_3 coated with copper. The peaks at 2θ=32.75, 35.58, 40.47 and 56.59 correspond to hematite (JCPDS Card No. 01-073-0603) phase in the material, to the planes (004), (110), (113) and (211) respectively (marked by * in the image). The peak at 2θ=73.28 (marked by # in the image) indicate existence of both Fe_2O_3 and copper (JCPDS Card No. 004-0836) phases. Thus, the XRD pattern confirms the coating of copper over Fe_2O_3 particles. The peaks in Figure 2, (b) at 2θ=43.60, 50.72 and 74.37 correspond to copper atoms

(JCPDS Card No. 00-003-1015) (marked by # in the image) and those at 2θ=44.94 and 82.47 correspond to iron atoms (JCPDS 00-001-1267), marked by $ in the image, thus, indicating the presence of both atoms.

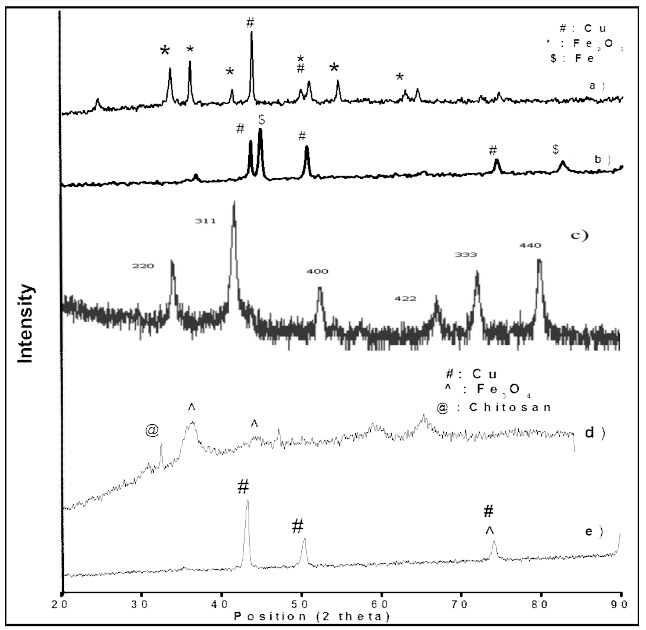

Figure 2: Represents XRD patterns of various Iron oxide composites: a) Fe_2O_3- Cu, b) Fe-Cu, c) Fe_3O_4, d) Fe_3O_4- CS, and e) Fe_3O_4-Cu.

In Figure 2, (c) shows the XRD pattern of magnetite particles. The peaks at 2θ values 30.3, 35.6, 43.1, 53.6 and 57.0 degree correspond to the plane (220), (311), (400), (422) ad (511) respectively. It confirms the presence of Fe_3O_4, and not γ-Fe_2O_3 (JCPDS Card no. 019-0629).

In Figure 2, (d) was the XRD image of chitosan coated with Fe_3O_4, with peak at 2θ=31.64 corresponding to chitosan (JCPDS Card No. 039-1894). Peaks at 2θ=37.87 and 65.74 refers to Fe_3O_4 (JCPDS Card No. 019-0629).

In Figure 2, (e) shows the XRD pattern of Fe_3O_4 coated with copper. The peaks at 2θ=43.07 and 50.08 correspond copper (JCPDS Card No. 04-0836) phase in the material, to the planes (111) and (200) respectively (marked by # in the image). The peak at 2θ=73.89 (marked by ^ in the image) indicate existence of both Fe_3O_4 (JCPDS Card No. 008-0087) and copper phases. Thus, the XRD pattern confirms the coating of copper over Fe_3O_4 particles.

FE-SEM analysis

Figure 3 represents FESEM images of all the samples along with EDX analysis. Figure 3, (a) shows the image of Fe_3O_4 coated with copper, with spherical shaped particles of size 55 μm (mean diameter). Figure 3, (b) shows Fe_2O_3 coated with copper, nano rod like particles with average length 220nm. Figure 3, (c) is Fe_3O_4 with non-uniform size of particles, varying from around 15 μm to 85 μm. In Figure 3, (d) depicts uniform sized Fe particles coated with copper particles, with average diameter of particles 150 μm. Figure 3, (e) is the image of Fe_3O_4- Chitosan beads were porous and spherical in shape; the average diameter of each bead is 377 μm.

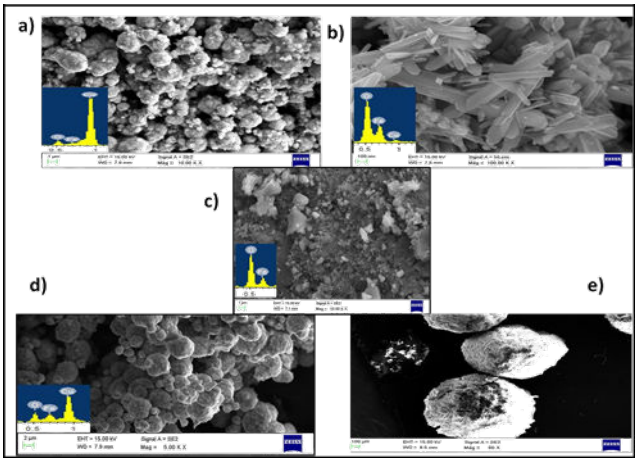

Figure 3: Shows FESEM images following composites a) Fe_3O_4- Cu; b) Fe_2O_3- Cu; c) Fe_3O_4; d) Fe-Cu; e) Fe_3O_4- Chitosan beads.

TEM analysis

The morphological and structural features of Magnetite chitosan nanocomposites were also characterised by transmission electron microscopy (TEM) coupled to an energy dispersive EDX microprobe and selected area electron diffraction (SAED) analysis. The size distribution histogram presented fairly monodispersed nanoparticles with the average size of 10-20 nm in good agreement. EDX spectra showed the chemical analysis of nanocrystals with Fe and chitosan (C, N, O) as the major elements (Figure 4).

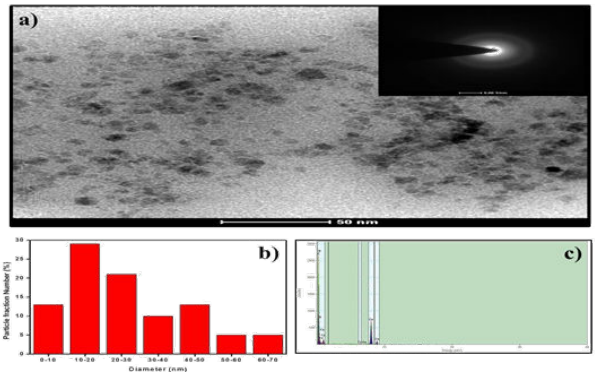

Figure 4: Represents TEM image of Fe_3O_4 Chitosan bead a) TEM image (inset: SAED image), b) particle size distribution histogram of Fe_3O_4 Chitosan beads and c) EDX spectrum.

Zeta potential analysis

Figure 5 shows zeta potentials of samples taken in their stable colloidal suspension at neutral pH: a) Fe_3O_4- Cu: -11.7 mV; b) Fe_2O_3-Cu: -16.1 mV; c) Fe_3O_4: 11.9 mV; d) Fe-Cu: -14.4 mV; e) Fe_3O_4-Chitosan: 19.1mV at acidic pH 5.5. The positive zeta potential of Fe_3O_4 chitosan is because of the presence of positively charged chitosan. The negative potential of copper coated nanocomposites may be attributed to the presence of copper.

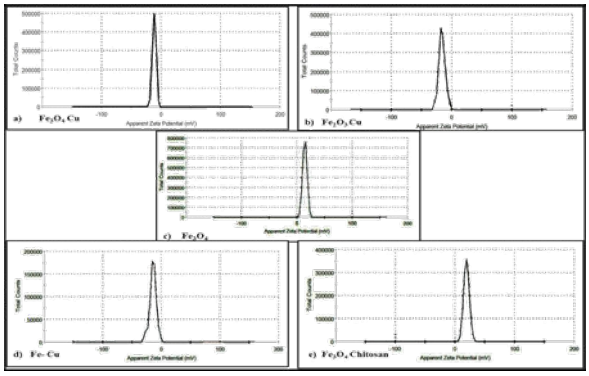

Figure 5: Represents Zeta potential of different a) Fe_3O_4- Cu, b) Fe_2O_3- Cu, c) Fe_3O_4, d) Fe-Cu and e) Fe_3O_4- Chitosan.

VSM analysis

Figure 6 depicts VSM images of all the samples. Zero coercivity indicates superparamagnetic nature of the sample. Magnetic saturation is observed at 1.08 emu/g, 0.8 emu/g, 0.77 emu/g, 0.64 emu/g and 0.54 emu/g respectively for Fe- Cu, Fe_3O_4, Fe_3O_4- Cu, Fe_3O_4- Chitosan and Fe_2O_3 - Cu. These values indicate that the samples have strong magnetic responsivity and can be easily separated from solution using magnetic field.

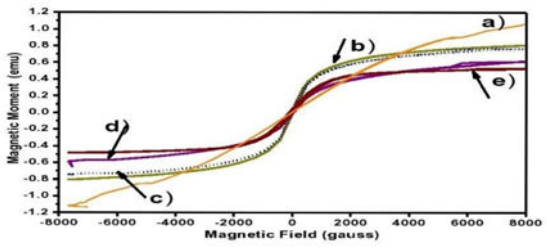

Figure 6: VSM image of a) Fe-Cu; b) Fe_3O_4; c) Fe_3O_4- Cu; d) Fe_3O_4-chitosan; and e) Fe_2O_3-Cu.

Sorption studies

0.1 g of Iron oxide nanocomposites was loaded with As (III)(0.5 mg/l) using 40 ml at pH 5.5 agitation period of 180 mins at RT and the agitation rate was 200 r/min. Adsorbed Iron oxide particles collected by magnetic device and was analysed by ICP-MS. The removal percent of As (III) in wastewater was calculated from the following equation:

$$\%Removal=1-m2/m1 \times 100$$

Where, m1 is the initial amount (mg) of As (III) and m2 is the amount (mg) of As (III) unadsorbed. The result of percent removal of As (III) by different Iron oxide composites were shown in Figure 7. After adsorption, among different iron oxide materials, chitosan magnetite bead was found to be higher in percentage removal of As (III) (93%).

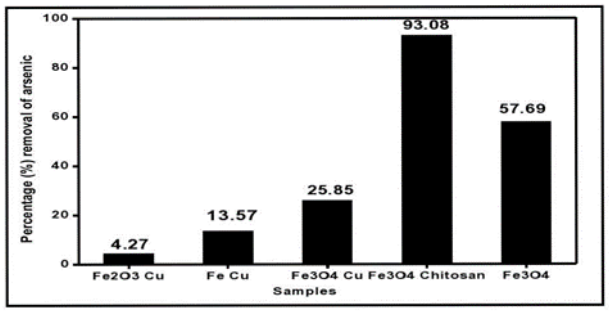

Figure 7: Graph represents the percentage (%) removal of As (III) by various iron oxide samples.

Antibacterial activity

We have investigated the biocidal action of different iron oxide nanocomposites. For this we considered *E.coli* and *S.aureus* as model bacteria and observed their growth in the presence of various iron oxide nanocomposites by spread plate method. For qualitative measurement, spread plate method was used. The nutrient agar was spread into the petri plate over the nanocomposites, the culture of both the bacteria's i.e gram positive and gram negative was spread on it. 5mg of each sample was taken and was incubated for 12 hours.

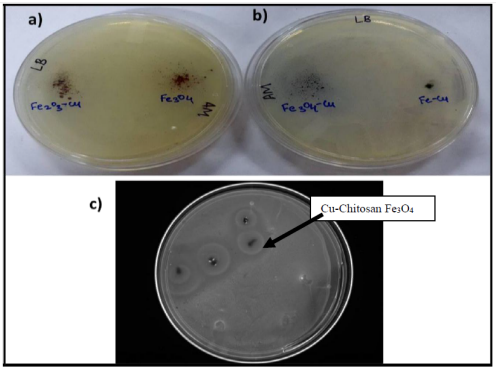

Figure 8: Showing the antibacterial effect of: a) Fe_2O_3- Cu and Fe_3O_4; b) Fe_3O_4- Cu and Fe-Cu; c) Fe_3O_4- Chitosan, using *E. coli* DH5α.

A marked difference was observed in the plates containing the Copper coated chitosan magnetite nanocomposite with a diameter of 1 cm as compared with the other iron oxide nanocomposites. This result is clearly evident in the Figure and, which confirms from zone of inhibition area that Cu coated Chitosan magnetite nanocomposites have strong inhibitory action against *E.coli* and *S.aureus* [24-26].

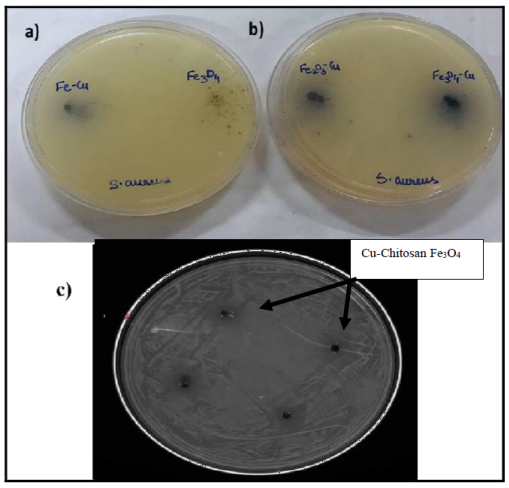

Figure 9: Showing the antibacterial effect of: a) Fe- Cu and Fe_3O_4; b) Fe_3O_4- Cu and Fe_3O_4-Cu; c) Fe_3O_4- Chitosan, using *S. aureus*.

Conclusion

Iron oxide nanocomposites were prepared for wastewater treatment. Adsorption occurs by exchange between OH_2 and -OH by As atoms in the coordination spheres of Fe atoms.

Chitosan contains many hydroxyl and amino functional groups, that act as adsorption sites for arsenic atoms. When dissolved in water, these amino groups gets deprotonated and bind with metal ions through chelation mechanism.

The best adsorption conditions are pH 5.5, adsorption time 180 mins, at RT. The used level was 0.1 g iron oxide nanocomposites added in 40 ml solution contained 0.5 mg/l As (III). The removal percent of As (III) from aqueous solution by magnetic chitosan beads was found to be 93%. It can be concluded that magnetic chitosan beads are an effective adsorbent for the removal of As (III) and microbes for the wastewater treatment.

Acknowledgements

The project was supported by Water Technology Initiative (WTI), Department of Science and Technology (DST), New Delhi. The author(s) would like to acknowledge their generous support.

References

1. Bissen M, Frimmel FH (2003) Arsenic-a Review. Part I: Occurrence, Toxicity, Speciation, Mobility. Acta Hydrochim. Hydrobiol 31: 9.
2. Twidwell LG, McCloskey J, Miranda P, Gale M, Gaballah I, et al. (1999) Proceedings of the Global Symposium on Recycling, Waste Treatment and Clean Technology, Warreandale, Pennsylvania, United States, p: 1715.
3. Hua M, Zhang S, Pan B, Zhang W, Lv L et al., (2012) Heavy metal removal from water / wastewater by nanosized metal oxides: A review. J Hazard Mater 212: 317-331.
4. Ergül B, Bektaş N, Öncel MS (2014) The Use of Manganese Oxide Minerals for the Removal Arsenic and Selenium Anions from Aqueous Solutions. Energy Environ 2: 103-112.
5. Suzuki TM, Bomani JO, Matsunaga H, Yokoyama T (2000) Preparation of porous resin loaded with crystalline hydrous zirconium oxide and its application to the removal of arsenic. React Funct Polym 43: 165-172.
6. Ouvrard S, Simonnot MO, Sardin M (2002) Reactive behavior of natural manganese oxides toward the adsorption of phosphate and arsenate. Eng Chem 41: 2785-2791.
7. Pena ME, Korfiatis GP, Patel M, Lippincott L, Meng X (2005) Adsorption of As(V) and As(III) by nanocrystalline titanium dioxide. Water Res 11: 2327-2337.
8. Ghimire KN, Inoue K, Makino K, Miyajima T (2002) Adsorptive Removal of Arsenic Using Orange Juice Residue. Sep Sci Technol 37: 2785-2799.
9. Wasiuddin NM, Tango M, Islam MR (2002) A Novel Method for Arsenic Removal at Low Concentrations. Energy Sour 24: 1031-1041.
10. Çiftçi TD, Henden E (2015) Nickel/nickel boride nanoparticles coated resin: A novel adsorbent for arsenic (III) and arsenic(V) removal. Powder Technol 269: 470-480.
11. Ali I, Othman ZA, Alwarthan A, Asim M, Khan TA (2014) Removal of arsenic species from water by batch and column operations on bagasse fly ash. Environ. Sci Pollut Res Int 21: 3218-3229.
12. Wang S, Gao B, Zimmerman AR, Li Y, Harris WG et al., (2015) Removal of arsenic by magnetic biochar prepared from pinewood and natural hematite. Bioresour Technol 175: 391-395.
13. Raven KP, Jain A, Loeppert RH (1998) Arsenite and Arsenate Adsorption on Ferrihydrite: Surface Charge Reduction and Net OH- Release Stoichiometry. Environ Sci Technol, p: 344.
14. Pierce ML, Moore CB (1981) Adsorption of Arsenite and Arsenate on Amorphous iron hydroxide from dilute aqueous solution. Water Res, p: 1247.
15. Gross PR, Eick M, Calvin CA, DL Sparks, Sabine G (1997) Arsenate and Chromate Retention Mechanisms on Goethite. 2. Kinetic Evaluation Using a Pressure-Jump Relaxation Technique. Environ Sci Technol 31: 321-326.
16. Manceau A (1995) The mechanism of anion adsorption on iron oxides: Evidence for the bonding of arsenate tetrahedra on free Fe (O, OH) 6 edges. Geochimica et Cosmochimica Acta 59: 3647-3653.
17. GA Waychunas, Rea BA, Fuller CC, Davis JA (1993) Surface chemistry of ferrihydrite: Part 1. EXAFS studies of the geometry of coprecipitated and adsorbed arsenate. Geochimica et Cosmochimica Acta 57: 2251-2269.
18. Arai K, Kinumaki T, Fujita T, Tokai B (1968) Toxicity of Chitosan. Reg Fish Res Lab, p: 89.
19. Konieczny J, Rdzawski Z (2012) Antibacterial properties of copper and its alloys. Mater Sci Eng 56: 53-60.
20. Anitha A, Divya VV, Krishna R, Sreeja V, Selvamurugan N, et al. (2009) Synthesis, characterization, cytotoxicity and antibacterial studies of chitosan, O-carboxymethyl and N,O-carboxymethyl chitosan nanoparticles. Carbohydr Polym 78: 672-677.
21. Huang SH, Liao MH, Chen DH (2003) Direct binding and characterization of lipase onto magnetic nanoparticles. Biotechnol Prog 19: 1095-1100.
22. Sharma R, Agarwala RC, Agarwala V (2006) Development of copper coatings on ceramic powder by electroless technique. Appl Surf Sci 252: 8487-8493.
23. Namdeo M, Bajpai SK (2008) Chitosan magnetite nanocomposites (CMNs) as magnetic carrier particles for removal of Fe(III) from aqueous solutions. Colloids Surf A Physicochem Eng Asp 320: 161-168.
24. Ahamed M, Siddiqui M, Akhtar MJ, Ahmad I, Pant AB et al. (2010) Genotoxic potential of copper oxide nanoparticles in human lung epithelial cells. Biochem Biophys Res Commun 396: 578-583.
25. Singh P, Bajpai J, Bajpai AK and Shrivastava BR (2011) Removal of arsenic ions and bacteriological contamination from aqueous solutions using chitosan nanospheres. Indian J ChemTechn 18: 403-413.
26. Elson CM, Davies DH, Hayes ER (1980) Removal of arsenic from contaminated drinking water by a chitosan/ chitin mixture. Water Res 14: 1307-1311.